Terahertz near-field imaging

2002 Phys. Med. Biol. 47 3727

(http://iopscience.iop.org/0031-9155/47/21/308)

INSTITUTE OF PHYSICS PUBLISHING PHYSICS IN MEDICINE AND BIOLOGY

Phys. Med. Biol. **47** (2002) 3727–3734 PII: S0031-9155(02)52609-9

Terahertz near-field imaging

John F Federici[1], Oleg Mitrofanov[1], Mark Lee[2], Julia W P Hsu[2], Igal Brener[2], Roey Harel[2], James D Wynn[2], Loren N Pfeiffer[2] and Ken W West[2]

[1] Department of Physics, New Jersey Institute of Technology, Newark, NJ 07102, USA
[2] Lucent Technologies, 600 Mountain Avenue, Murray Hill, NJ, USA

Received 26 March 2002
Published 17 October 2002
Online at stacks.iop.org/PMB/47/3727

Abstract

A near-field probe is described that enables high spatial resolution imaging with terahertz (THz) pulses. The spatial resolution capabilities of the system lie in the range of few microns and we demonstrate a resolution of 7 μm using broad-banded THz pulses with an intensity maximum near 0.5 THz. We present a study of the performance of the near-field probes in the collection mode configuration and discuss some image properties.

1. Introduction

Spectroscopy and imaging technology has progressed rapidly into the THz region of the electromagnetic spectrum during the last few years [1]. This advance is mostly due to development of the THz time-domain (or THz time-resolved) spectroscopy (THz-TDS) technique [2, 3]. This method covers a wide spectral window from 0.1 THz to 40 THz, which is rich in electromagnetic phenomena. The THz-TDS system has a small power in the THz beam, but exceptional sensitivity. This combination makes the system a powerful tool for far-infrared imaging [4–7] and spectroscopy [8, 9]. In this paper, we summarize our development of an imaging method that provides a very high spatial resolution and has all the advantages of the THz-TDS technique [15]. Furthermore, we discuss its applications to THz measurements of biological imaging.

The major limitation of THz imaging is poor spatial resolution due to the long THz wavelength. The resolution can be significantly improved by implementing the concept of near-field scanning optical microscopy. Various methods based on this approach have been demonstrated, pushing the resolution limit to a few tens of microns [10–15, 17]. Among them is a dynamic aperture approach that potentially can improve resolution to a few microns [14, 16]. However, application of this method is limited to semiconductor surfaces and images are related to the concentration of photogenerated carriers. In an alternative approach, a micromachined near-field probe was fabricated [17]. This device, with a spatial resolution of a few tens of microns, is capable of mapping the propagation of THz pulses on coplanar transmission lines. Unlike near-field probes that are predicated on THz transmission through small apertures and exhibit a cut-off frequency in the THz, near-field probes based on coaxial

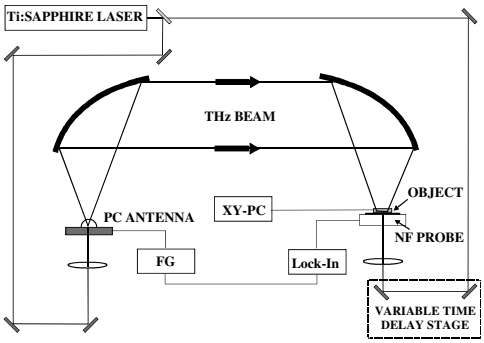

Figure 1. Schematic diagram of the THz near-field imaging set-up (XY-PC denotes *xy*-position control equipment for scanning and FG—a function generator, which applies the alternating bias to the PC antenna).

transmission lines do not exhibit a cut-off. In fact, the spatial resolution is primarily determined by the physical dimension of the centre coaxial conductor. By modifying a scanning force microscopy probe with a coaxial metal shield, van der Weide demonstrated submicron spatial resolution with 1.4–2 GHz microwave signals [18].

Imaging of biological samples with THz has shown great promise. The simplest form of THz imaging is the contrast due to the strong absorption of water [19, 20]. One advantage of THz-TDS is the ability to distinguish chemicals and biochemicals via their spectroscopic signatures or optical properties (e.g., index of refraction) in the THz range. For example, it has been demonstrated that THz transmission measurements can be used to identify the binding state of DNA molecules through the change in its complex index of refraction [21].

The resolution capabilities of our THz near-field method [15, 22, 23] lie in the range of a few microns, which is considerably smaller than the wavelengths of the employed THz radiation (250–1500 μm). High spatial resolution in imaging can be achieved if the evanescent components of the field scattered by the object are detected. The evanescent field exists only at the object and decays very fast with increasing distance from it. Detection of the evanescent field is possible by introducing an aperture-type probe into the near-field region of the object. Fields in front of the aperture determine waves that couple into the probe. These waves carry information about the point of the object where the probe is placed. By scanning the object in front of the probe one constructs a near-field image. The spatial resolution of this method is defined by the aperture size and is not limited by diffraction. Furthermore, the resolution is independent of the THz wavelength. The combination of the near-field microscopy concept with the THz-TDS technique allows studying of the temporal evolution of the electromagnetic field in the near field of objects.

2. Experimental set-up

The near-field probe is an essential element of the system. The probe makes use of an efficient design that allows the detection of the electric field coupled through an aperture as small as $\lambda/300$. The THz near-field imaging set-up is presented in figure 1. THz pulses are generated by the transient current in a photoconducting (PC) switch excited by optical pulses from a mode-locked Ti–sapphire laser ($\lambda_c = 800$ nm, $\tau_{FWHM} = 150$ fs). The repetition rate of the laser system is 100 MHz. The THz beam is focused on the object through a transparent substrate by means of two off-axis parabolic mirrors. The beam waist in the object plane is $\sim$2 mm (FWHM), which is usually much larger than the object, therefore the illumination can

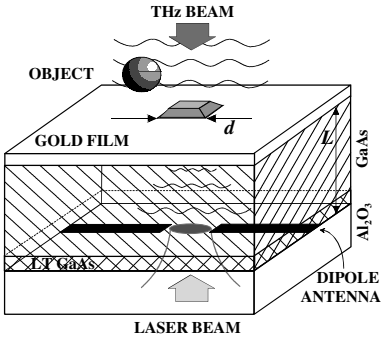

Figure 2. Schematic diagram of the near-field probe.

be considered uniform. The near-field probe is located behind the sample, almost in contact with the object. The probe consists of a small aperture in a metallic screen and a PC antenna that detects THz pulses. Generation of the THz pulses is slowly modulated by applying a square wave alternating bias to the emitting PC switch. The detecting antenna is gated by optical pulses from the same laser. Current induced in the antenna is proportional to the THz field and is measured using a lock-in amplifier.

An automated xy-translation stage scans an object perpendicular to the optical axis. A variable time delay stage allows time-domain sampling of the THz pulse. The image is constructed using the THz signal collected either at a fixed time delay or in the time domain for every position. A part of the set-up including the THz transducers, THz optics and the object, is enclosed into a vapour-tight box purged with nitrogen gas to reduce absorption and dispersion due to water vapour.

A schematic diagram of the near-field probe is presented in figure 2. An entrance subwavelength aperture of size d (5–50 μm) is lithographically defined on a surface of the probe in a 600 nm gold film evaporated on a thinned GaAs layer. A GaAs protrusion through the aperture enhances field coupling into the probe. The PC planar antenna is embedded between a thin layer of GaAs (3–10 μm, $n \sim 3.6$) and a sapphire substrate ($n \sim 3.1$). Note that the space behind the aperture is filled with a high refractive index material that reduces the effective wavelength. The antenna is fabricated on a 1 μm thick low temperature grown GaAs epilayer. Details of the probe fabrication are described elsewhere [23]. The sapphire substrate supports the structure and allows the optical gating pulses access the antenna from the substrate side.

3. Near-field probe

3.1. Probe sensitivity

Most of the incident THz power is reflected from the metallic screen, and transmission through a subwavelength aperture is extremely small [24]. The electric field that exists behind the illuminated subwavelength aperture can be divided into modes with real and imaginary longitudinal k-vectors [25]. The latter are usually referred to as evanescent modes. Electric field amplitude of the evanescent modes is significantly larger than that of the propagating modes at distances from the aperture $z < d/2$ [26]. At a distance approximately equal to the aperture size, their contribution is comparable. As the distance z increases, the amplitude of both mode types decreases, but decay is much more rapid in the case of the evanescent

modes, which do not transfer energy into the far-field region. Only the modes with real wavenumbers can propagate to distances $z \gg \lambda$. Therefore evanescent modes are not detected in conventional collection mode near-field microscopy. An important feature of our probe design is that the electric field that couples through the aperture is detected inside the probe in the near-field zone of the aperture ($z < d/2$). Therefore, not only propagating but also evanescent modes of the radiation transmitted through the aperture contribute to the signal. Detection of the evanescent modes of the aperture results in a higher sensitivity of the near-field probe [15, 23].

3.2. Resolution

The spatial resolution of the near-field probe is defined by the aperture size. To demonstrate it, we performed an edge resolution test on the probes with different aperture sizes. Boundary conditions for the electric field at a metallic edge are different for the two principal polarizations (parallel and perpendicular to the edge). If the edge is oriented parallel to the polarization of the incident THz pulse, then the electric field in the plane of the object exhibits a sharp contrast between the metallic and the open areas [27]. These tests reveal a 7 μm spatial resolution for a 5 μm aperture probe ($L = 4$ μm) when the edge is scanned over the probe at a distance $h \sim 2$ μm. The resolution test on the probes with larger apertures showed that spatial resolution scales with the aperture size and is independent of wavelength [15].

Electric fields with high spatial frequency only exist in the proximity of the object (evanescent fields) and decay over distances comparable to the size of object features. In order to detect these fields, the near-field probe must be placed very close to the object. The fast decay of the high spatial frequency fields is observed when performing an edge test for various separations between the probe and the object, h. The sharp edge profile smears as h increases. In practical THz near-field imaging, the probe–sample separation is less than several microns. Waveform distortion due to interference is negligible at this range, however the variation of the amplitude of the detected THz field can create an uneven background in the image, if the separation is not maintained constant during the scan.

The resolution test on the probes with larger apertures showed that spatial resolution scales with the aperture size. Spatial resolution in near-field microscopy is independent of wavelength. We measured time-domain waveforms for every position of the edge with respect to the aperture. The amplitude of a particular frequency component of the THz pulse is obtained by applying Fourier transform to the time-domain data. Figure 3 shows the edge profile at various frequencies measured using the 10 μm aperture probe ($L = 4$ μm). Identical resolution curves are obtained for a wide spectral window (0.2–2.5 THz), limited only by the noise level.

3.3. Aperture size

One of the limiting factors that restrict using very small apertures for high resolution is the substantial reduction of the transmitted power as the aperture size decreases. According to the Bethe–Bouwkamp [28, 29] theory of transmission through a subwavelength aperture, electric field amplitude of the transmitted radiation decreases as the third power of the aperture size. The transmission coefficient is also frequency dependent and, therefore, the near-field probe exhibits a non-uniform frequency response due to the aperture. The transmission coefficient of the aperture decreases as ω^2 for frequencies smaller than the cut-off frequency of the aperture [28]. Therefore the spectral content of the detected pulse shifts to higher frequencies as the aperture size decreases. The THz pulse amplitude decreases as d^3 as the aperture size d is decreased.

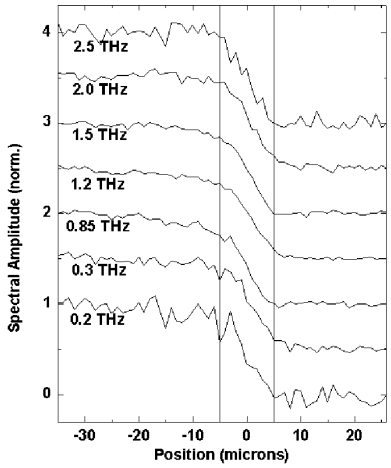

Figure 3. A spatial resolution of 10 μm is independent of frequency as demonstrated using the near-field probe with $d = 10$ μm and $L = 4$ μm.

3.4. Probe–sample separation

Another effect related to the probe–sample separation is interference of the waves reflected by the probe and the sample surfaces. This effect results in a variation of the detected field as a function of the probe–sample separation. The metallic surface of the near-field probe reflects the incident THz field toward the sample surface, at which the pulse partially reflects and eventually falls on the probe again. The consequent reflections are detected by the probe at time delays, corresponding to multiple double-paths between two surfaces. If the probe–sample separation is larger than half the length of the THz pulse in free space, then the reflections can be easily distinguished in the time domain. As the probe–sample separation decreases, the reflections start to overlap, distorting the pulse waveform. When the sample–probe separation is smaller than $\sim$15 μm (the delay between reflections is $<$0.1 ps), the reflections overlap constructively and the waveform is almost indistinguishable from that of the incident pulse, but the waveform amplitude increases as distance h decreases. This effect is not related to the evanescent field and is completely described by interference [15].

4. Image properties

It should be emphasized that the near-field image of an object is not a direct replica of the instantaneous electric field scattered by the object. The probe aperture alters the detected waveform. In principle, the original waveform can be extracted if the transfer function of the aperture is known. Analysis of THz near-field image formation appears as the essential task in order to apply this technique. In this respect, we would like to mention the finite-difference time-domain numerical method [23, 30, 31], which can be used to simulate THz near-field images.

The THz-TDS technique allows studying objects in the time domain and/or frequency domain. These images provide a wealth of spatial and spectral information if full THz waveforms are recorded at each spatial position. As an example of the near-field probe's imaging ability, the series of images in figure 4 demonstrates changes of the image pattern with time. At various time slices, the interaction between the near-field THz and the object vary. The object in this experiment is a gold dipole antenna embedded in a planar transmission

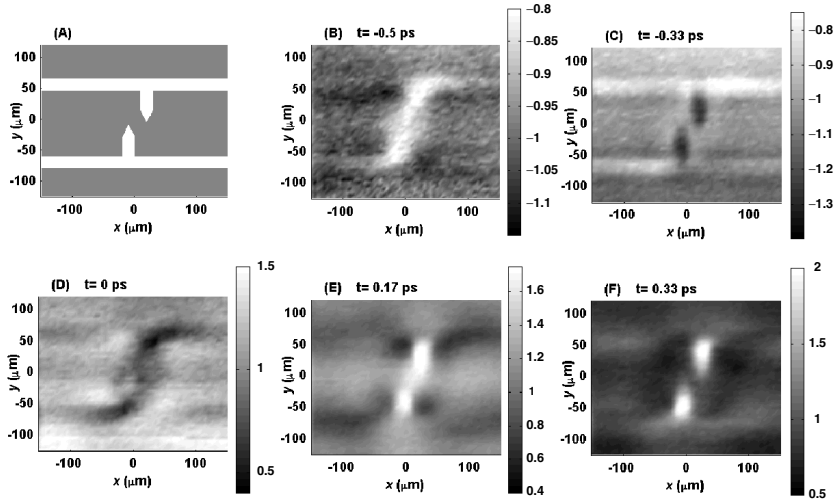

Figure 4. (A) Schematic diagram of a planar antenna on sapphire. (B)–(F) Series of near-field images taken at different time delays of the gating optical pulse. The grey level corresponds to the measured electric field.

line. The antenna is lithographcally printed on a sapphire substrate and consists of two sharp ended 50 μm long arms, slightly shifted with respect to each other, and two 20 μm wide striplines separated by 105 μm. A schematic diagram of the antenna is shown in figure 4(A). The object contains only gold features oriented either parallel to the direction of polarization (dipole arms) or perpendicular to it (strip lines). The images are obtained at consequent moments in time using the 10 μm aperture probe ($L = 4$ μm).

Contrary to continuous wave illumination, when an image pattern is stationary, images recorded using single-cycle pulses vary in time since the response of the object features to the short pulse of THz is time-dependent. Frames (B) ($t = -0.5$ ps) and (D) ($t = 0$) correspond to the negative and positive peaks of the pulse waveform. The images are similar except for polarity. The dipole creates a shadow due to absorption by metal in the centre. The shadow extends slightly towards the striplines, which exhibit weaker contrast in these images.

All object features develop well in frame (C) ($t = -0.33$ ps), which corresponds to a moment between the negative and positive peaks of the THz pulse. Both the striplines and the dipole arms are clearly seen. However, the object parts oriented perpendicularly to the polarization direction appear brighter and the parts oriented parallel to it appear darker with a higher contrast. Resolution is comparable in both directions. Frames (E) ($t = 0.17$ ps) and (F) ($t = 0.33$ ps) show another effect. The dipole arms are imaged as bright spots with high contrast. Both images correspond to the positive time delay, when the background electric field amplitude has already decreased.

It is informative to consider time-domain waveforms measured at various points of the object. One can see an obvious perturbation of the electric field due to the dipole. A waveform measured at the dipole area shows a larger amplitude and delayed phase, compared to a waveform measured away from the antenna. Therefore the dipole appears glowing after the peak of the incident pulse has passed ($t \sim 0.2$–0.5 ps).

Clearly, the 7 μm spatial resolution of near-field THz makes is difficult to resolve the structure of a cell unless the size of the cell is larger than 7 μm [20]. One application of near-field THz imaging to biological samples would be the imaging of thin sections of tissues.

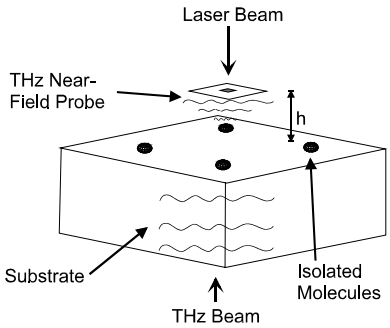

Figure 5. Schematic illustration of using THz near-field probe to measure THz image of isolated biomolecules on a 'biochip'.

As noted previously, the near-field tip must be scanned within a few microns of the sample surface and the sample thickness should be no more than about 10 μm thick to maintain the best spatial resolution. For this application, the contrast in the tissue image would be determined by differences in water absorption or other absorption differences for different tissue areas (e.g., cancerous or normal areas of tissue). Another implementation of THz near-field imaging would be to measure the THz optical properties or spectra of isolated biomolecules. Since the 7 μm spatial resolution is not sufficient to isolate an individual molecule within a cell or culture, it would have to be physically isolated from other biomolecules as shown in figure 5. In this 'biochip' configuration [21], the advantage of near-field THz is that isolated biomolecules could be measured with more THz radiation interacting with the biomolecules as compared to the far-field.

5. Conclusion

Near-field imaging at THz frequencies has developed into a reliable tool with spatial resolution of a few microns. Significant improvement of resolution over the diffraction limit is possible because of an efficient near-field probe design and the exceptional sensitivity of the THz-TDS technique. The spatial resolution is independent of THz frequency and only depends on the aperture size. Using time-resolved measurements two types of THz near-field images can be constructed: (a) time-domain frames of electric field, and (b) chromatic images (amplitude and phase). The latter method opens the possibility for near-field spectroscopy at THz frequencies. The image acquisition time in this case will increase considerably, since a complete time-domain waveform is measured for every pixel. For biological samples, THz near-field imaging could find use in imaging thin biological tissues or as a diagnostic tool for biochips.

Acknowledgment

JFF would like to thank Professor J M Joseph for many stimulating discussions.

References

[1] Mittleman D M, Gupta M, Neelamani R, Baraniuk R G, Rudd J V and Koch M 1999 Recent advances in terahertz imaging *Appl. Phys.* B **68** 1085–94

[2] Nuss M C and Orenstein J 1998 Terahertz time-domain spectroscopy *Millimeter-Wave Spectroscopy of Solid (Springer Topics in Applied Physics, vol 74)* ed G Gruner (Berlin: Springer)
[3] van Exter M and Grischkowsky D R 1990 Characterization of an optoelectronic terahertz beam system *IEEE Trans. Microw. Theory Tech.* **38** 1684–91
[4] Hu B B and Nuss M C 1995 Imaging with terahertz waves *Opt. Lett.* **20** 1716–9
[5] Han P Y, Cho G C and Zhang X-C 2000 Time-domain transillumination of biological tissues with terahertz pulses *Opt. Lett.* **25** 242–4
[6] Mickan S, Abbott D, Munch J, Zhang X-C and Van Doorn T 2000 Analysis of system trade-offs for terahertz imaging *Microelectron. J.* **31** 503–14
[7] Han P Y, Cho G C and Zhang X-C 2000 Time-domain transillumination of biological tissues with terahertz pulses *Opt. Lett.* **25** 242–4
[8] Federici J F, Greene B I, Dykaar D R, Sharifi F and Dynes R C 1992 Direct picosecond measurement of photoinduced Cooper pair breaking in lead *Phys. Rev.* B **46** 11153
[9] Saeta P, Federici J F, Greene B I and Dykaar D R 1992 Intervalley scattering in GaAs and InP probed by far infrared absorption spectroscopy *Appl. Phys. Lett.* **60** 1477
[10] Hunsche S, Koch M, Brener I and Nuss M C 1998 THz near-field imaging *Opt. Commun.* **150** 22–6
[11] Wynne K and Jaroszynski D A 1998 Superluminal terahertz pulses *Opt. Lett.* **24** 25–7
[12] Mitrofanov O, Brener I, Harel R, Wynn J D, Pfeiffer L N, West K W and Federici J 2000 Terahertz near-field microscopy based on a collection mode detector *Appl. Phys. Lett.* **77** 3496–8
[13] Mitrofanov O, Brener I, Wanke M C, Ruel R R, Wynn J D, Bruce A J and Federici J 2000 Near-field microscope probe for far infrared time domain measurements *Appl. Phys. Lett.* **77** 591–3
[14] Chen Q, Jiang Z, Xu G X and Zhang X-C 2000 Near-field terahertz imaging with a dynamic aperture *Opt. Lett.* **25** 1122–4
[15] Mitrofanov O, Lee M, Hsu J W P, Brener I, Harel R, Federici J, Wynn J D, Pfeiffer L N and West K W 2001 Collection mode near-field imaging with 0.5 THz pulses *IEEE J. Sel. Top. Quantum Electron.* **7** 600
[16] Chen Q and Zhang Z C 2001 Semiconductor dynamic aperture for near-field terahertz wave imaging *Sel. Top. Quantum Electron.* **7** 608
[17] Lee H, Lee J and Kim J 2001 A micromachined photoconductive near-field probe for picosecond pulse propagation measurement on coplanar transmission lines *IEEE J. Sel. Top. Quantum Electron.* **7** 674
[18] van der Weide D W 1997 Localized picosecond resolution with a near-field microwave/scanning-force microscope *Appl. Phys. Lett.* **70** 677
[19] Hu B B and Nuss M C 1995 Imaging with terahertz waves *Opt. Lett.* **20** 1716
[20] Han P Y, Cho G C and Zhang X-C 2000 Time-domain transillumination of biological tissues with terahertz pulses *Opt. Lett.* **25** 242
[21] Brucherseifer M, Nagel M, Bolivar Haring P, Kurz H, Bosserhoff A and Buttner R 2000 Label-free probing of the binding state of DNA by time-domain terahertz sensing *Appl. Phys. Lett.* **77** 4049
[22] Mitrofanov O, Lee M, Hsu J W P, Pfeiffer L N, West K W, Wynn J D and Federici J F 2001 Terahertz pulse propagation through small apertures *Appl. Phys. Lett.* **79** 907
Mitrofanov O, Brener I, Harel R, Wynn J D, Lee M and Federici J 2000 Far-infared near field microscopy based on a collection mode detector *Appl. Phys. Lett.* **77** 3496
Mitrofanov O, Brener I, Wanke M C, Ruel R R, Wynn J D, Bruce A J and Federici J 2000 Near-field microscope probe for far infrared time domain measurements *Appl. Phys. Lett.* **77** 591
[23] Mitrofanov O, Harel R, Lee M, Pfeiffer L N, West K, Wynn J D and Federici J 2001 Study of single-cycle pulse propagation inside a THz near-field probe *Appl. Phys. Lett.* **78** 252
[24] Wynne K, Carey J J, Zawadzka J and Jaroszynski D A 2000 Tunneling of single-cycle terahertz pulses through waveguides *Opt. Commun.* **176** 429–35
[25] Grober R D, Rutherford T and Harris T D 1996 A modal approximation for the electromagnetic field of a near-field optical probe *Appl. Opt.* **35** 3488–95
[26] Bethe H A 1944 Theory of diffraction by small holes *Phys. Rev.* **66** 163
[27] Brener I, Hunsche S, Cai Y, Nuss M C, Wynn J, Lopata J and Pfeiffer L 1998 Time resolved near field imaging and diffraction with subwavelength far-infrared dipole sources *Ultrafast Phenomena XI* pp 171–2
[28] Bethe H A 1944 Theory of diffraction by small holes *Phys. Rev.* **66** 163–82
[29] Bouwkamp C J 1950 On Bethe's theory of diffraction by small holes *Philips Res. Rep.* **5** 321–32
[30] Taflove A and Hagness S 2000 *Computational Electrodynamics: The Finite-Difference Time-Domain Method* (Boston, MA: Artech House Publishers)
[31] Bromage J, Radic S, Agrawal G P, Stroud C R, Fauchet P M Jr and Sobolevski R 1998 Spatiotemporal shaping of half-cycle terahertz pulses by diffraction through conductive apertures of finite thickness *J. Opt. Soc. Am.* B **15** 1399–405